Mechanochemical dehydrochlorination and chelation reaction in the solid state: from a molecular salt to a coordination complex†

Fang Guo,*[a] Hui-de Shao,[a] Qi Yang,[a] Antonino Famulari[b] and Javier Martí-Rujas*[bc]

Solid-state chemistry offers the opportunity to study intriguing chemical reactions, providing insights into their mechanisms.[1] Mechanochemical synthesis,[2,3] where two or more solids react induced by mechanical energy (*i.e.*, manual grinding or ball milling) is becoming a powerful method to study the solid state reactivity of pharmaceutical cocrystals,[4] the ionic interconversion in molecular salts,[5] and the synthesis of metal–organic frameworks.[6]

Dehydrochlorination reactions consisting of the removal of HCl from crystalline salts are one type of solid-state reaction that has been rarely investigated in coordination molecular complexes.[7,8] Only recently such reactions have been monitored by heating or mechanical grinding. So far, the dehydrochlorination reactions studied have used small cations (pyridinium or imidazolium) and tetrachlorometallate (II) anions $[MCl_4]^{2-}$.[9]

The sequestration of metal ions by chelating functional groups such as ethylenediamine has been used in supramolecular chemistry to prevent the formation of extended networks (*i.e.*, coordination polymers) and to promote the formation of discrete structures.[10] Reports showing the mechanochemical

transformation from hydrogen bonded networks into coordination complexes *via* dehydrochlorination followed by chelation are uncommon.

Herein, we have used mechanochemistry to monitor the solid-state reactivity of flexible bidentate ligand N,N,N',N'-tetra-*p*-methoxybenzyl-ethylenediamine (**L**) possessing an ethylenediamine core and flexible arms, with $CuCl_2 \cdot 2H_2O$ (Scheme 1). We describe the mechanochemical formation of salt $[H_2L]^{2+} \cdot [CuCl_4]^{2-}$ (**1**) and its transformation to a new discrete neutral metal coordination complex $[(CuCl_2)(L)] \cdot 2(H_2O)$ (**2**·$2H_2O$) *via* a dehydrohalogenation reaction. We demonstrate that the ionic molecular complex transforms into a neutral metal complex where two charge-assisted Cu–Cl···H–N hydrogen bonds are substituted by two new Cu–N coordination bonds through chelation by the ethylenediamine core of ligand **L**. The by-product H_2O molecules are incorporated in the crystal structure and play an important role maintaining the crystallinity. Quantum mechanics (QM) were carried out to understand the electronic density distribution of frontier orbitals in ligand **L** using the structural models obtained from single crystal X-ray determination.

To the best of our knowledge this is the first reported example of chelation after dehydrohalogenation reaction monitored by mechanochemical means.

For the mechanochemical synthesis of **1**, ligand **L** (540 mg : 1 mmol) was protonated by adding 100 µL of HCl (37%) to yield the salt $[H_2L]Cl_2$, and then ground with $CuCl_2 \cdot 2H_2O$ (170 mg : 1 mmol) for one minute using a mortar and pestle. During the reaction, we observed a color change from white to an intermediate green that transforms to orange, indicating the formation of new phase **1** (Fig. S1†). The quantitative

[a] College of Chemistry, Liaoning University, Shenyang 110036, China.
E-mail: fguo@lnu.edu.cn; Fax: +86 24 62202380; Tel: +86 24 62207831

[b] Dipartimento di Chimica Materiali e Ingegneria Chimica "Giulio Natta",
Politecnico di Milano, Via L. Mancinelli 7, 20131 Milan, Italy. E-mail: javier.rujas@iit.it;
Fax: +39 2399 9866; Tel: +39 2399 9890

[c] Center for Nano Science and Technology@Polimi, Istituto Italiano di Tecnologia,
Via Pascoli 70/3, 20133 Milano, Italy
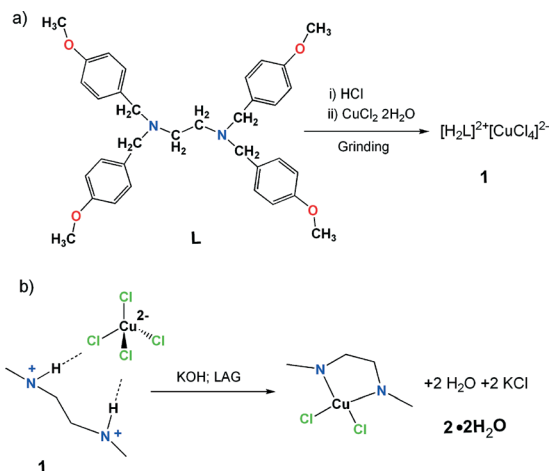
Scheme 1 Cartoon depicting (a) the synthesis of salt **1**, and (b) its dehydrochlorination and chelation reaction by liquid assisted grinding to form **2·2H₂O**.

Fig. 2 Comparison of XRPD patterns of **2·2H₂O**: from simulated XRPD (top), recrystallized product from methanol of the phase generated by grinding (center), and the crude product (including product phase, KCl, bottom).

formation of **1** was confirmed by X-ray crystallography and elemental analysis. Single crystals suitable for X-ray diffraction were obtained from solution mixing of diprotonated H_2L and $CuCl_2·2H_2O$ in concentrated HCl. The match between the measured X-ray powder diffraction (XRPD) on the polycrystalline **1** obtained after grinding and that simulated from single crystal X-ray diffraction data indicates that the structures are the same (Fig. S2†).

The structure of salt **1** was reported in ref. 11 and is composed of 0.5 $[CuCl_4]^{2-}$ dianions and 0.5 doubly protonated **L** in each asymmetric unit. The $[CuCl_4]^{2-}$ dianions are hydrogen bonded with diprotonated H_2L through N–H···Cl and C–H···Cl interactions yielding a "clamp-shaped" building block unit. The building block units are further linked by weak C–H···Cl interactions to give linear chains along the *b*-axis (Fig. 1).[11] We note that the stoichiometric water in the $CuCl_2·2H_2O$ is not included in the structure, nor is atmospheric water.[12] Due to the orientation of the $[CuCl_4]^{2-}$ anions towards the N atoms in the backbone of the ligand (Fig. 1a), it is reasonably speculated that following a dehydrochlorination reaction, salt complex **1** could transform into a coordination complex if hydrogen bonds were broken and new Cu–N coordination bonds were formed. Therefore, we used mechanochemistry to study that reaction in the solid state.
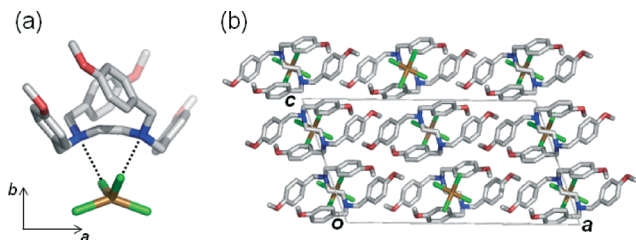

Fig. 1 (a) The hydrogen bonding interactions between dianion and dication through N–H···Cl interactions are shown as dashed lines. (b) Packing along the *b*-axis in **1**. Colour code: carbon (grey); nitrogen (blue); oxygen (red); copper (brown); chloride (green).
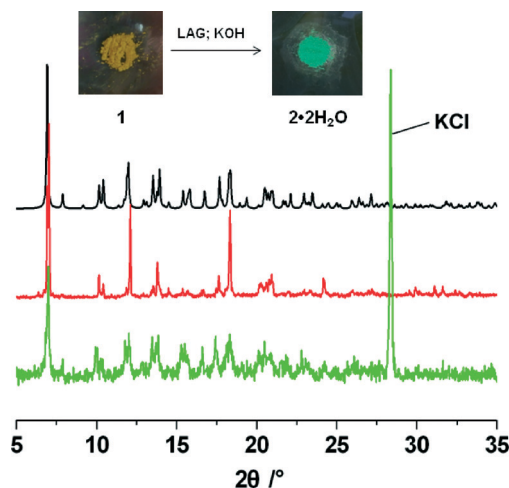
Liquid assisted grinding (LAG)[13] of **1** and KOH in a 1 : 2 molar ratio, with the addition of 30 µl of methanol, was carried out. Upon grinding, a color change from orange to dark green was observed over a few minutes. XRPD of the powder product indicated that a new phase and the generation of by-product KCl (2θ 28°) had been formed (Fig. 2). In the reaction the presence of KOH promotes the dehydrochlorination, forming two by-product KCl and H_2O molecules. We note that neat grinding of **1** and KOH did not lead to the formation of new products; only a mechanical mixture of the starting materials was observed by XRPD. In this case, the catalytic activity of the solvent is necessary for the reaction to occur. The new crystalline phase generated by grinding was recrystallized from methanol, yielding suitable crystals for single crystal X-ray diffraction analysis. The good match between the XRPD pattern obtained by grinding and that simulated from single crystal X-ray data (Fig. 2) suggests that the bulk powder has the same structure as the one obtained from the single crystal.

Single crystal X-ray structure determination confirms that salt **1** transformed to the neutral metal coordination complex $[(CuCl_2)(L)]·2(H_2O)$ (**2·2H₂O**) after dehydrochlorination.‡§ During the transformation from **1** to **2·2H₂O**, new Cu–N coordination bonds were formed while disruption of non-covalent N–H···Cl hydrogen bonds took place (Fig. 3). It is noted that the space group is maintained (*C2/c*) after the dehydrochlorination, whereas the main changes in the lattice parameters correspond
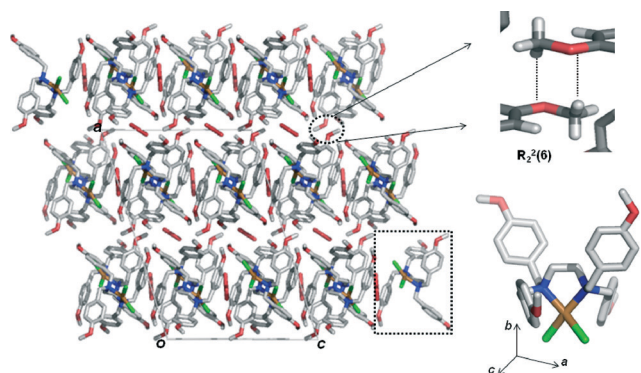
Fig. 3 Crystal packing of **2**·2H$_2$O along the *b*-axis showing the segregation of methoxybenzyl pendant groups which interact with each other *via* hydrogen bonds. Water molecules are shown in red. Colour code as in Fig. 1. Top inset: view of the $R_2^2(6)$ hydrogen bond interactions. Hydrogen bond interactions are shown as dashed lines. Bottom inset: stick representation showing the clamp-shaped ML unit with the Cu–N coordination bonds in **2**·2H$_2$O.

to the *b*- and *c*-axis, which are the axes along which the [CuCl$_4$]$^{2-}$ dianions are hydrogen bonded to diprotonated ligand. Water molecules, most likely generated in the reaction, are trapped and involved in the stabilization of the crystal structure of **2**·2H$_2$O.

Upon dehydrohalogenation of salt **1**, ligand **L** chelates the Cu metal, forming a five-membered ring. In **2**·2H$_2$O the copper atoms adopt a tetrahedral coordination with two N atoms of ligand **L** and two Cl atoms.[14,15] After coordination, the conformation of ligand **L** remains essentially unchanged, and the 'clamp-shaped' ligand geometry observed in **1** is maintained (Fig. 3).

In **2**·2H$_2$O, the ML units (where ML = [(CuCl$_2$)(L)] are hydrogen bonded with the included water molecules *via* Cl···O interactions[16] (Fig. S3†). One of the pendant methoxybenzyl groups links to a neighbour ML unit *via* C–H···O interactions (C13–H13c···O1: 3.447 Å, 134.0°) in $R_2^2(6)$ mode forming 1D chains (Fig. 3 and S3†). Of the three remaining pendant methoxybenzyl groups, two are engaged in weak hydrogen bonding interactions forming the 3D structure *via* C–H···O interactions (C16–H16A···O3: 3.394 Å, 137.0° and C20–H20A···O1: 3.588 Å, 165.7°) (Fig. S3 and S4†). The protruding fourth methoxybenzyl group does not interact with surrounding groups, which explains its disordered nature. The segregation into domains where methoxybenzyl groups interact with neighbour molecules is notable, a feature that is also observed in **1**.

Thermogravimetrical analysis of **2**·2H$_2$O shows that the complete removal of H$_2$O is achieved around 240 °C corresponding to a weight loss of 5.62% (calc. 5.67) (Fig. S5†). The XRPD pattern reveals that significant changes in peak positions occurred upon heating **2**·2H$_2$O to 65 °C *in vacuo* for 2 h; however, the crystallinity was lost after heating **2**·2H$_2$O to 90 °C for 2 h, yielding an amorphous phase (Fig. S7†). Thermal treatment can also induce the removal of HCl gas and the formation of a coordination complex;[7b] however, in the present case, heating of **1** did not lead to the formation of **2**·2H$_2$O.

To further study the reverse reaction, (*i.e.*, from the metal coordination complex to hydrogen bonded salt), we have performed a solid–gas experiment in which the dehydrated phase was introduced into a sealed vessel containing concentrated HCl and placed in equilibrium with its vapour for 3 weeks (Fig. S7†), and found that the evacuated phase exhibits an irreversible behaviour in contact with vapours of HCl.[17]

To rationalize the different solid state stabilities of **1** and **2**·2H$_2$O observed experimentally, we have carried out QM calculations in the solid state. In particular density functional theory (DFT) calculations, employing both the PWC (Perdew–Wang)[18] and the PBE (Perdew–Burke–Ernzerhof)[19] exchange–correlation functions, have been performed. A combination of numerical double-ζ quality basis set (including polarization functions on all atoms, *i.e.*, DNP) and effective core potential was chosen. We assumed experimental X-ray determined geometries for heavy atoms optimizing only X–H bond lengths. The same computational approach was proved to be adequate in a number of cases such as large supramolecular complexes,[20] systems containing charged particles[5b,21,22] and crystalline phases of thiophene based oligomers and polymers.[23] All the calculations were accomplished by the DMol^3 software.[24]

DFT calculations in the solid phase show that the hydrated phase in the coordinated complex **2**·2H$_2$O is more stable than the anhydrous one, suggesting that the included water molecules template the structure. Up to 6% of the total unit cell volume corresponds to voids (pockets) generated after manually removing the water molecules.[25] Thus, the release of water molecules upon heating is not facilitated by continuous channels, and most likely major molecular rearrangements leading to an amorphous phase take place when the water is lost.

Any chemical reaction accompanied by the disruption of some chemical bonds and generation of new bonds can lead to the change of the energies of reactants and products. DFT provides an ideal method to monitor such changes. We carried out QM calculations (gas phase) to obtain the electron density of frontier orbitals in **L**, taking into account the structure of **L** in **1** and **2**·2H$_2$O in an attempt to get insights on the reaction. PBE/DNP calculations show that upon protonation, the electron distribution of the HOMO in **1** is surrounding the benzene rings (π-orbitals) as shown in Fig. 4. Upon deprotonation, (*i.e.*, after the removal of 2H$^+$ and 2Cl$^-$ ions) QM calculations show that the more reactive part is localized along the chelating N–C–C–N backbone in **L**. In fact, the electron distribution of the HOMO is substantially different in the coordinated ligand in which all the electron distribution is localized at the N atoms. Moreover, the energy of the deprotonated ligand **L** is higher than that of **1** and **2**·2H$_2$O (Fig. 4). Additionally, the QM calculations show that the diprotonated ligand in **1** is *ca.* 50 kcal mol^{-1}, more stable than the coordinated conformation. Interestingly, the stabilities observed by QM (Fig. 4) show the same trend as the experimental melting points of **L** (69 °C), **2**·2H$_2$O (108 °C) and **1** (159 °C).

Although we have used a quite raw approximation using QM calculations in the gas phase approximation, some insights into the frontier molecular orbital distribution accounting for
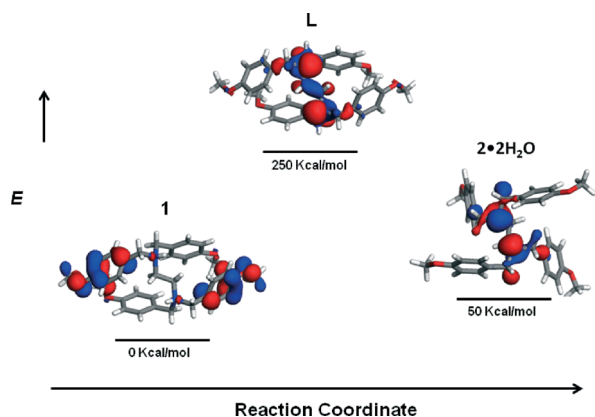
Fig. 4 Plot showing the calculated HOMO orbitals corresponding to different conformations of bidentate ligand in **1**, **2·2H₂O** and **L**. From the computed energies, the most stable is the charge assisted salt **1**, followed by the coordinated complex **2·2H₂O** with the least stable the neutral ligand **L**.

the behaviour of the flexible bidentate ligand during the mechanochemical dehydrochlorination reaction have been achieved.

In summary, we have reported a solid-state mechanochemical transformation from a molecular salt into a discrete coordination complex *via* a dehydrohalogenation reaction using a large and flexible chelating ligand. The reported process is one of the first examples where a dehydrohalogenation reaction is followed by chelation of the diethylamine group in the backbone of an organic ligand. DFT calculations were used to attempt a rationalisation of the structural transformation from a hydrogen bonded complex salt into a coordination complex. We are currently investigating dehydrohalogenation reactions using different metal halides, bases and ligands including mechanistic aspects by means of *ex situ* or *in situ* X-ray powder diffraction.

Acknowledgements

References

1 (*a*) G. M. H. Schmidt, *Pure Appl. Chem.*, 1971, **27**, 647; (*b*) K. Tanaka and F. Toda, *Chem. Rev.*, 2000, **100**, 1025; (*c*) G. K. Kole and J. J. Vittal, *Chem. Soc. Rev.*, 2013, **42**, 1755; (*d*) P. Naumov, Chemical X–Ray Photodiffraction: Principles, Examples, and Perspectives *Top. Curr. Chem.*, 2012, **315**, 111; (*e*) F. Guo, J. Martí-Rujas, Z. Pan, C. E. Hughes and K. D. M. Harris, *J. Phys. Chem. C*, 2008, **112**, 19793; (*f*) M. Garai, R. Santra and K. Biradha, *Angew. Chem., Int. Ed.*, 2013, **52**, 5548; (*g*) J. Martí-Rujas, N. Islam, D. Hashizume, F. Izumi, M. Fujita and M. Kawano, *J. Am. Chem. Soc.*, 2011, **133**, 5853; (*h*) A. Peuronen, A. Valkonen, M. Kortelainen, K. Rissanen and M. Lahtinen, *Cryst. Growth Des.*, 2012, **12**, 4157; (*i*) J. Martí-Rujas and M. Kawano, *Acc. Chem. Res.*, 2013, **46**, 493.

2 (*a*) S. L. James, C. J. Adams, C. Bolm, D. Braga, P. Collier, T. Friščić, F. Grepioni, K. D. M. Harris, G. Hyett, W. Jones, A. Krebs, J. Mack, L. Maini, A. G. Orpen, I. P. Parkin, W. C. Shearouse, J. W. Steed and D. C. Waddell, *Chem. Soc. Rev.*, 2012, **41**, 413; (*b*) T. Friščić, *Chem. Soc. Rev.*, 2012, **41**, 3493.

3 T. Friščić, A. V. Trask, W. Jones and W. D. S. Motherwell, *Angew. Chem., Int. Ed.*, 2006, **45**, 7546.

4 S. Karki, T. Friščić, W. Jones and W. D. S. Motherwell, *Mol. Pharmaceutics*, 2007, **4**, 347.

5 (*a*) L. Loots, H. Wahl, L. van der Westhuizen, D. A. Haynes and T. le Roex, *Chem. Commun.*, 2012, **48**, 11507; (*b*) F. Guo, M.-Q. Zhang, A. Famulari and J. Martí-Rujas, *CrystEngComm*, 2013, **15**, 6237.

6 K. Fujii, A. L. Garay, J. Hill, E. Sbircea, Z. Pan, M. Xu, D. C. Apperley, S. L. James and K. D. M. Harris, *Chem. Commun.*, 2010, **46**, 7572.

7 (*a*) G. M. Espallargas, L. Brammer, J. Van de Streek, K. Shankland, A. J. Florence and H. Adams, *J. Am. Chem. Soc.*, 2006, **128**, 9584; (*b*) C. J. Adams, H. M. Colquhoun, P. C. Crawford, M. Lusi and A. G. Orpen, *Angew. Chem., Int. Ed.*, 2007, **46**, 1124; (*c*) E. Coronado, M. Giménez-Marqués, G. M. Espallargas and L. Brammer, *Nat. Commun.*, 2012, **3**, 828.

8 (*a*) C. J. Adams, M. A. Kurawa, M. Lusi and A. G. Orpen, *CrystEngComm*, 2008, **10**, 1790; (*b*) C. J. Adams, A. L. Gillon, M. Lusi and A. G. Orpen, *CrystEngComm*, 2010, **12**, 4403; (*c*) C. J. Adams, M. F. Haddow, M. Lusi and A. G. Orpen, *CrystEngComm*, 2011, **13**, 4324.

9 C. J. Adams, M. F. Haddow, R. J. I. Hughes, M. A. Kurawa and A. G. Orpen, *Dalton Trans.*, 2010, **39**, 3714.

10 (*a*) M. Fujita, J. Yazaki and K. Ogura, *J. Am. Chem. Soc.*, 1990, **112**, 5645; (*b*) M. Fujita, D. Oguro, M. Miyazawa, H. Oka, K. Yamaguchi and K. Ogura, *Nature*, 1995, **378**, 469.

11 F. Guo, M. Q. Zhang, N. Lu, J. Tong, H. Y. Guan and B. X. Wang, *CrystEngComm*, 2011, **13**, 6753.

12 We note that atmospheric water can be easily incorporated in the crystal structure during mechanochemical reactions. See ref. 5*b*.

13 LAG refers to the mechanical reaction aided by the addition of stoichiometric amounts of solvent.

14 The bond lengths of Cu–N are 2.060(3) Å and 2.069(3) Å, whereas the bond lengths of Cu–Cl being 2.249(2) Å and 2.250(1) Å.

15 We note that the methoxyl groups of **L** are disordered, with the C and O atoms of each methoxyl group displaying higher thermal parameters; in addition, one methoxyl group and its attached benzene ring were refined anisotropically over two positions with the occupancies given as 0.50/0.50.

16 The short contacts are: (Cl1···O5w: 3.09(1) Å; Cl2···O1w: 3.188(9) Å).

17 Although it has been shown that dehydrochlorination reactions in some cases are reversible, an irreversible transformation has also been reported. See ref. 7*b*.

18 J. P. Perdew and Y. Wang, *Phys. Rev. B: Condens. Matter Mater. Phys.*, 1992, **45**, 13244.

19 (*a*) J. P. Perdew, K. Burke and M. Ernzerhof, *Phys. Rev. Lett.*, 1996, **77**, 3865; (*b*) J. P. Perdew, K. Burke and M. Ernzerhof, *Phys. Rev. Lett.*, 1997, **78**, 1396.

20 (*a*) Y. Kolokoltsev, O. Amelines-Sarria, T. Y. Gromovoy and V. A. Basiuk, *J. Comput. Theor. Nanosci.*, 2010, **7**, 1095; (*b*) O. Amelines-Sarria, Y. Kolokoltsev and V. A. Basiuk, *J. Comput. Theor. Nanosci.*, 2010, **7**, 1996; (*c*) V. A. Basiuk, O. Amelines-Sarria and Y. Kolokoltsev, *J. Comput. Theor. Nanosci.*, 2010, **7**, 2322; (*d*) V. A. Basiuk, *Int. J. Quantum Chem.*, 2011, **111**, 4197.

21 G. Yu, S. Yin, Y. Liu, Z. Shuai and D. Zhu, *J. Am. Chem. Soc.*, 2003, **125**, 14816.

22 (*a*) E. Maccaroni, L. Malpezzi, A. Famulari and N. Masciocchi, *J. Pharm. Biomed. Anal.*, 2012, **60**, 65; (*b*) M. Casalegno, A. Baggioli, A. Famulari, S. V. Meille, T. Nicolini, R. Po and G. Raos, Materials for organic photovoltaics: insights from detailed structural models and molecular simulations *EPJ Web Conf.*, 2012, 02002, DOI: 10.1051/epjconf/20123302002, ISSN 2100-014X; (*c*) A. Baggioli, S. V. Meille, G. Raos, R. Po, M. Brinkmann and A. Famulari, *Int. J. Quantum Chem.*, 2013, **113**, 2154.

23 A. Famulari, G. Raos, A. Baggioli, M. Casalegno, R. Po and S. V. Meille, *J. Phys. Chem. B*, 2012, **116**, 14504.

24 B. Delley, *J. Chem. Phys.*, 2000, **113**, 7756; Materials Studio and DMOL[3] are Accelerys Inc. products (see http://www.accelrys.com).

25 A 1.2 Å probe radius was used to determine the solvent accessible area using Mercury 3.1 software.